ACS Macro Letters

Letter

pubs.acs.org/macroletters

Crystallization of thin polymer layers confined between two adsorbing walls

Bram Vanroy,[†] Michael Wübbenhorst,[†] and Simone Napolitano*[,‡]

[†]Laboratory of Acoustics and Thermal Physics, Department of Physics and Astronomy, KU Leuven, Celestijnenlaan 200D, Leuven, 3001, Belgium

[‡]Laboratory of Polymer and Soft Matter Dynamics, Faculté des Sciences, Université Libre de Bruxelles (ULB), Boulevard du Triomphe, Bâtiment NO, Bruxelles 1050, Belgium

Supporting Information

ABSTRACT: Confined at the nanoscale level, polymers crystallize much slower than in bulk, and in some cases, the formation of ordered structure is inhibited within extremely long experimental time scales. Here, we report on the thickness dependence of the conversion rate of the amorphous fraction of ultrathin films of poly(ethylene terephthalate) during isothermal cold crystallization. We present a new analytical method assessing the impact of irreversible chain adsorption and permitting to disentangle finite size and interfacial effects. From the μm range down to a few tens of nm, we observed an increase in crystallization time scaling with the inverse of the film thickness, which is a fingerprint of finite size effects. Films thinner than ~20 nm did not crystallize, even after prolonged annealing in the temperature range where the crystallization rate reaches its maximum value. Noticing that this threshold corresponds to the total thickness of the layer irreversibly adsorbed within our investigation time, we explain these findings considering that chain adsorption increases the entropic barrier required for the formation of crystalline structures.

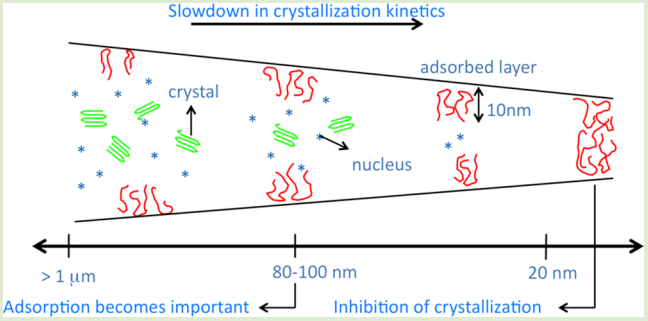

Polymers do not crystallize easily. Due to their complex molecular architecture, in fact, organization in ordered structures is permitted only in the case of stereoregular chains, and the increase in molecular size further complicates the complex mechanism of chain folding required to form polymer crystals. Like for smaller molecules,[1] crystallization becomes even more sluggish when the chains are confined at the nanoscale level,[2] where different morphologies are observed,[3] the overall crystallization rate is reduced by several orders of magnitude,[4−6] and, in some cases, crystallization does not occur within the experimental time scale.[7] Focusing on ordering, the slowing-down in the kinetics is commonly related to both the finite value of the nuclei density and to the reduced mass transport in proximity of an interface. The origin of the latter phenomenon is still unclear. Some authors attributed it to slower interfacial segmental dynamics,[7,8] some others attributed it to less efficient diffusion of material toward the crystallization front in films thinner than the lamellar thickness. The particular geometry used in the experiments does not permit a straightforward discrimination between the two hypotheses. Thin polymer layers are, in fact, spincoated onto a solid substrate, and the presence of the free surface (in contact with air or vacuum) perturbs the structural dynamics,[9] introducing an asymmetric, not well-defined, profile of mobility.

To overcome this issue, in this study we focused on films of poly(ethylene terephthalate), PET, a system widely investigated in bulk[10,11] and, upon confinement,[12−15] with symmetric boundary conditions provided by identical polymer−metal (aluminum) interfaces. Though metallization of the upper surface did not allow investigation by surface methods such as optical and scanning probe microscopies, measurement of the current flow generated upon application of an AC electric field perpendicular to the surface of the films permitted us to study the crystallization kinetics via dielectric spectroscopy. Based on our observation, we explain the slower crystallization rate in the thinner films in terms of an entropic barrier related to chain adsorption.

Following our previous work,[16−18] we exploited the correlation between the dielectric strength, $\Delta\varepsilon$, that is, the dielectric dispersion correlated to the structural process, and the density number of relaxation units participating to the structural process. In isothermal conditions, in fact, $\Delta\varepsilon$ corresponds to the contribution to the dielectric constant given by the orientational polarization and is proportional to the number of dipole moments able to fluctuate on the time scale of the relaxation time, τ. Owing to such a direct link, we could monitor the cold crystallization kinetics (that is, crystallization of an amorphous sample above and in the

Received: December 12, 2012
Accepted: January 31, 2013
Published: February 5, 2013

   dx.doi.org/10.1021/mz300641x | ACS Macro Lett. 2013, 2, 168−172

vicinity of its glass transition temperature) in ultrathin organic films down to a few tens of nanometers via the gradual immobilization of the amorphous fraction, resulting in a detectable drop in $\Delta\varepsilon$. Furthermore, we demonstrated that this approach permits the following of the formation of irreversibly adsorbed layers[19,20] and the estimation of the gradient of mobility introduced by interfacial interactions.[21,22]

Ultrathin films were prepared by spincoating solutions of PET in a mixture (5:2) of triflouroacetic acid and chloroform. Metallization of the upper and lower surface of the organic layer (aluminum 99%, pressure $<10^{-6}$ mbar, evaporation rate $\geq$10 nm s^{-1}, thickness ~50 nm; contact with air, before spincoating, favors the formation of a layer of 2−3 nm of oxide on top of the metal, which enhances the affinity with PET, yielding an interfacial energy[16] of 3.0 mJ·m^{-2}) permitted the preparation of nanocapacitors (area = 4 mm^2) for dielectric relaxation experiments. Previous work[23] verified that in this geometry both the segmental mobility profile (τ) and the gradient in orientational polarization ($\Delta\varepsilon$) are symmetric with respect to the center of the film.

In the thickness range considered (10 nm to 10 μm), the crystallization rate varies by more than 5 orders of magnitude. To investigate all the samples at the same crystallization temperature, experiments were performed at 373 K, where the characteristic crystallization time, t_{cry}, is ~7 min in bulk samples. At the chosen temperature, the structural relaxation process of PET appears as a strong peak in $\varepsilon''(f)$, the imaginary component of the dielectric function, centered around 10 kHz (for bulk, that is, $\tau \sim 16$ μs). The intensity of the structural peak ($\Delta\varepsilon$) decreased during isothermal annealing, implying chain immobilization, see Figure 1.

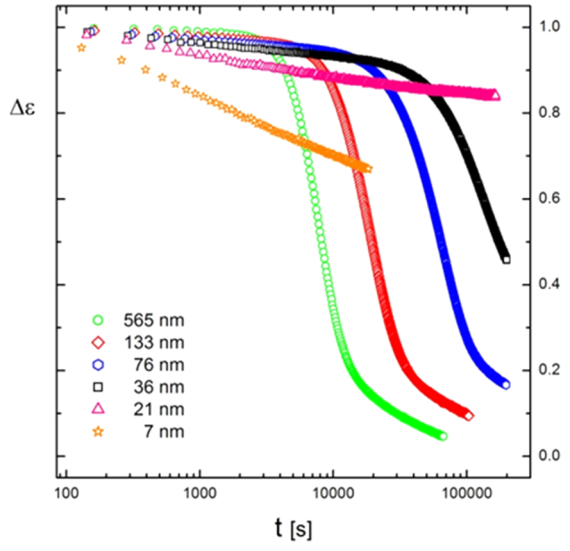

Figure 1. Time evolution of the dielectric strength of films of PET of different thicknesses, capped between aluminum layers.

A straightforward analysis of this reduction allowed us to disentangle crystallization and adsorption events. Both types of kinetics can be described by exponential functions of the type $\Delta\varepsilon(t) \sim 1 - \exp(-t/t_{cry})^{\beta}$, where the exponent β provides information on the dimensionality and/or cooperative nature of the kinetics. In the case of adsorption, β assumes values between 0 and 1 (stretched exponential), while β is larger than unity (<4, compressed exponential) for crystallization kinetics following the Avrami equation. Interfacial rearrangements increasing the monomer/surface density without affecting the thickness of the adsorbed layer yield a further drop in $\Delta\varepsilon$, scaling logarithmically with the annealing time.[20] Consequently, focusing on primary crystallization and adsorption, we analyzed the overall time evolution of the dielectric strength as

$$\frac{\Delta\varepsilon(t)}{\Delta\varepsilon(t_0)} = 1 - \Gamma[1 - \exp(t/t_{cry})^{\beta}] - \delta \log(t/t_0) \quad (1)$$

where Γ indicates the final drop in dielectric strength (proportionally to the crystalline content of the sample), δ is a parameter proportional to the fraction of chains immobilized upon adsorption, and t_0 is a conveniently short time that we fixed for all samples at 1 s. Furthermore, we determined the induction time, t_N, related to the onset of the larger reduction in dielectric strength. The results of our analysis are plotted in Figure 2. β dropped continuously down to a couple of tens of nanometers, from ~3 (μm range) to 1.5 (~20 nm). Consequently, the reduction of $\Delta\varepsilon$ was mainly due to crystallization.

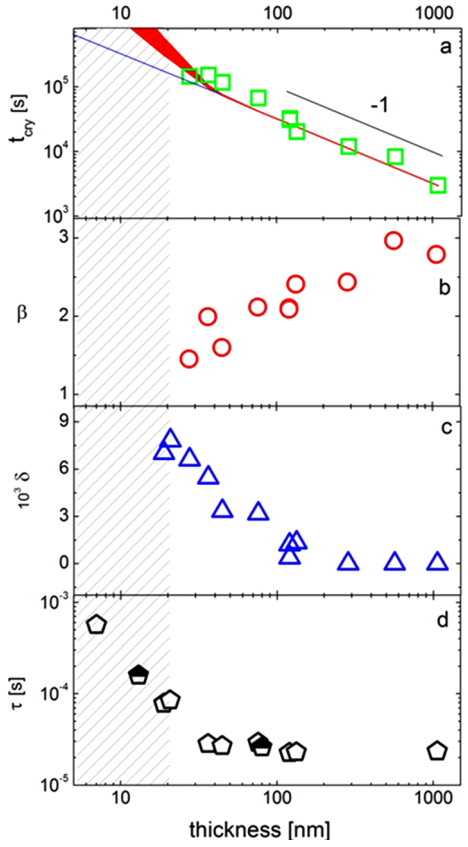

Figure 2. Thickness dependence of the fitting parameters of crystallization time (a), Avrami exponent (b), and adsorption coefficient (c), as obtained from the fit of the time evolution of the dielectric strength via eq 1. The values of the structural relaxation time of amorphous films at 373 K were also plotted (d). In (a), the red area indicates the values of crystallization time, as obtained via eq 2, where ξ was varied between 1 and 0.5; the blue line refers to the expected increase in t_{cry} due to finite size effects. In (d), data from ref 12 were added for comparison (semi-open symbols). The shadow area below 20 nm indicates the thickness range where crystallization was not observed.

dx.doi.org/10.1021/mz300641x | ACS Macro Lett. 2013, 2, 168−172

Similar smooth changes were observed for t_{cry} and t_N (see Supporting Information); on the contrary, δ showed an abrupt reduction around 130 nm. In particular, while for thicker films the dielectric strength remained unaffected by annealing at $t < t_N$, below this thickness range we observed a progressive increase in $|d\Delta\varepsilon/d \log(t)|$ at $t \ll t_N$, that is, in δ. In our previous work, we assigned the value of this quantity to rearrangements in the adsorbed layer, aiming at maximizing the enthalpic gain upon adsorption.[20] This observation is in line with literature showing that crystallization can take place in previously adsorbed layers.[24] We can consider the largest thickness where $\delta > 0$ as an upper limit for the impact of interfacial interactions. Remarkably, this value is in excellent agreement with the length scale estimated analyzing the thickness dependence of the structural relaxation of PET,[22] ~120−150 nm (=2 × 68 ± 7 nm).

As anticipated, in proximity of this thickness we did not see any perturbation in the conversion of the amorphous fraction. However, in line with the trends in supported films, also in case of capped films, we observed that the crystallization kinetics tremendously slowed down upon confinement. In particular, here we found that the values t_N and t_{cry} increased with the inverse of the film thickness. Considering that the surface of the samples was kept constant, those trends reveal a strong dependence of the crystallization kinetics on the volume. A similar result was observed in nanodroplets of poly(ethylene oxide), PEO,[25,26] and corresponds to a nucleation-limited slowing down in the crystallization kinetics. Assuming a constant nuclei density, reduction of the thickness yields, in fact, a lower probability to find active nuclei that could start the phase transition. Such hypothesis, further supported by a similar continuous and unperturbed reduction of β, is in line with the prediction of the finite-size corrections proposed to the Avrami model.[27] In the case of a finite volume, in fact, the presence of interfaces does not permit a full development of the crystals as in bulk and contribution of trunked crystals and lost nuclei (belonging to region outside the volume considered) results in a lower effective transformation rate and smaller values of β.[28]

For films thinner than $h^* \sim 20-25$ nm, we could not detect any substantial reduction in dielectric strength imputable to crystallization. This observation implies that, in this thickness regime, the crystallization rate decreased by more than 3 orders of magnitude or that crystallization was definitely inhibited. The same results were reproduced in experiments at higher temperatures where the crystallization kinetics is intrinsically sped up by the larger diffusion coefficients and in repeated temperature scans up to T_m + 20 K where T_m is the bulk melting point, see Supporting Information. It is noteworthy mentioning that, regardless of the type of polymer/substrate interactions, the presence of an interface can only reduce the value of T_m.[29] Further measurements via X-ray reflectivity confirmed that a 15 nm thick film of PET capped between Al layers does not crystallize after an annealing of 24 h at 453 K, which is the temperature showing a maximum in crystal growth rate in bulk (~75 nm/s).[30]

The observations collected so far are in clear disagreement with conjectures on the impact of interfacial segmental mobility on the crystallization kinetics. Previous work speculated that the increase in t_{cry} should be related to a smaller growth rate due to the slower interfacial dynamics, that is, larger values of τ.[5,7,8,31] Our approach permitted to finally clarify this point. The correlation between t_{cry} and τ originates from the Stoke−Einstein relation,[16,32] providing a link between rotational and translation modes. In particular, assuming that all the changes in the crystallization time are related to a perturbation in the structural dynamics, we can write

$$\frac{\tau(h)}{\tau(h_0)} = \Lambda(h)\left[\frac{t_{cry}(h)}{t_{cry}(h_0)}\right]^{\xi} \quad (2)$$

where h_0 is a reference thickness, $\Lambda(h)$ is a term introduced to take into account of nucleation effects, and ξ is the fractional Stokes−Einstein coefficient, assuming values typically between 1.0 and 0.5. To check the validity of this scaling, we considered the thickness dependence of the structural relaxation time at t_0, that is, in the amorphous state; τ remained constant down to h^* and finally increased in the thinner films, in line with previous investigation of PET,[12] see Figure 2d. We started by considering the case that the change in crystallization rate are totally imputable to slower interfacial relaxation, that is, $\Lambda(h) \equiv 1$.

This condition implies a thickness independent crystallization time down to h^*. Already at this thickness, t_{cry} exceeds by more than 2 orders of magnitude the values measured in the μm range, which finally disproves the hypothesis that the reduction in crystallization kinetics are merely due to slower structural relaxation. We have then included the impact of nucleation, mimicking the effects observed for $h > h^*$, that is, $\Lambda(h) \sim h^{-1}$. Under this condition, at thicknesses where we have not measured any crystallization event, t_{cry} would instead assume values detectable by our experimental approach. Consequently, we verified that the combination of finite size effects on nucleation and the longer relaxation times in proximity of the metallic interfaces cannot justify the tremendous drop in crystallization rate for $h < h^*$.

We considered two other possible contributions. In supported films, a severe reduction of crystal growth rate was experimentally observed for i-PS when the thickness of the sample was reduced below the lamellar size, l_C; such a trend was later confirmed by simulations of polymer melts.[33,34] In these conditions, thickening of lamellar crystals is highly hindered by the lack of material and the longer paths needed to transport new chain to the growth front. Given the symmetry of our sample, we can expect a similar transition at thicknesses exceeding $L^* = 2l_C + l_a$, where l_a is the thickness of the amorphous layer in between lamellae. In fact, the concurrent formation of a lamella at each polymer/metal interface retards crystal growth due to the hindrance exerted by the amorphous layer in between the two ordered structures. For samples of PET of the same source used in this work, at 373 K, l_C = 2.9 nm and l_a = 3.9 nm,[35] providing a lower limit of 10 nm ($<h^*$), which is compatible with the experimental threshold value.

Alternatively, we took into account the impact of the formation of an irreversible adsorbed layer[36,37] (Guiselin brush[38]) on crystallization. As noticed by the nonzero values assumed by δ below 130 nm, thermal annealing in the liquid state ($T > T_g$) promotes the adsorption of PET onto Al. Following our previous work on polystyrene,[19,20] we monitored the irreversible adsorption kinetics of PET, verifying the equivalence between the time dependence of the thickening of the Guiselin brush and the drop in dielectric strength during isothermal experiments (see Figure 3 and Supporting Information). We isolated the irreversibly adsorbed layer from 40 nm thick films held at 373 K for different annealing times. For this thickness, at the chosen annealing temperature,

dx.doi.org/10.1021/mz300641x | ACS Macro Lett. 2013, 2, 168−172

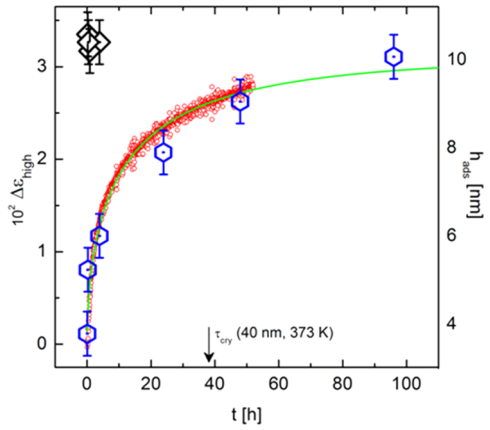

Figure 3. Time evolution of the component of the dielectric strength with higher decaying rate, $\Delta\varepsilon_{high}$ (red circles, left axis), and the thickness of the irreversibly adsorbed layer, h_{ads}, obtained in the same annealing conditions (blue hexagons, right axis) at 363 K. Value of h_{ads} collected under the isothermal crystallization conditions, 373 K, are shown for comparison (black diamonds, right axis).

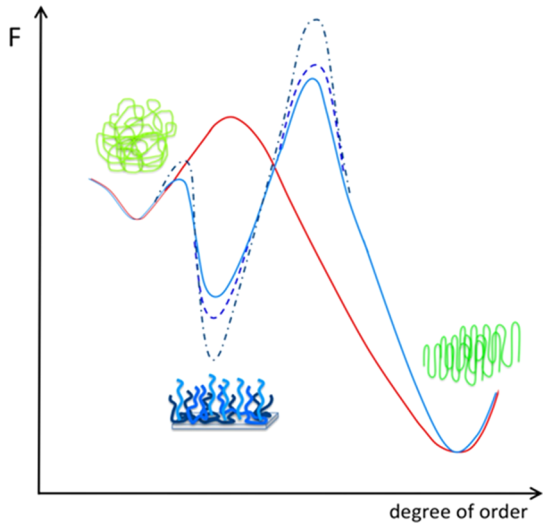

Figure 4. Sketch of the changes in free energy as a function of the degree of order for a semicrystalline polymer in proximity of an adsorbing interface. Far from the interface (red curve), a reduction of free energy (F) requires overcoming an activation barrier related to the formation of stems. Following Ostwald's rule of stages, interfacial chains prefer to get adsorbed onto the substrate, passing through the metastable state with smallest difference in F. However, upon adsorption, the reduction in free energy increases the depth of the energy barrier to overcome before crystallization.

$t_N = 10h$ and $t_{cry} = 42h$. After already 10 min the thickness of the adsorbed layer reached a constant value, implying that adsorption takes place already before the onset of crystallization, in line with the trends in Figure 1.

To analyze more carefully the adsorption kinetics we performed further experiments at 363 K, where crystallization did not take place during the whole measurement time (~96 h) and the adsorption kinetics is slower. The results show the same trend observed in other polymers, that is a fast growth saturating at long annealing times. The thickness h_f reached after 4 days was comparable to the values found at 373 K after ~10 min. We could fit the data at 363 K with an exponential curve of the type $h_{ads}(t) = h(0) + h_f[1 - \exp(-t/t_{ads})]$, where $h_f = 10.0 \pm 1.2$ nm, $t_{ads} \sim 10^5$ s, and built up the dimensionless parameter $t^* = t_{ANN}/t_{ads}$, a useful probe of confinement effects.[19,20] The trends at the two different annealing temperatures confirmed that during our crystallization experiments, the onset of crystallization, corresponded to $t^* \gg 1$, that is, $t_{ads} < t_N$, for all the thicknesses investigated. Previous work revealed that, when this condition is reached, the deviations from bulk behavior do not depend sensitively on the annealing time, that is, a new well-defined steady state is achieved. Moreover, in this regime, due to a potential barrier exerted by chains that have already been pinned onto the substrate, adsorption of new chains is accompanied by a severe entropic penalty.[39,40] Due to the lesser available space, the number of possible conformations permitting adsorption at this stage is strongly limited. We expect that at $t^* \gg 1$, the crystallization of chains in the irreversibly adsorbed layer is highly hindered. Although ordering yields a remarkable gain in enthalpy, the formation of crystals requires an initial entropic loss[41] that cannot be outweighted by the adsorbed chains. The restriction in conformational degrees of freedom due to chain pinning, in fact, leads to an increase in the entropic barrier of stem formation, see Figure 4. For those systems where crystallization starts after reaching the regime $t^* \gg 1$ (e.g., for low M_w polymers), we expect a severe reduction in the overall crystallization rate of ultrathin films, in correspondence of the thickness of the irreversibly adsorbed layer reached during the experiment, $\sim h_f$. We noticed that the $h^* \approx 2h_f$ (in our geometry two adsorbing interfaces are present), which validates our hypothesis.

In this framework, the formation of an irreversibly adsorbed layer in semicrystalline polymers can be treated via the Ostwald rule of stages,[42] see Figure 4, via a series of transformations through metastable states with close free energies. Irreversible chain adsorption does not, however, ensure thermodynamic equilibrium.[43] The conformations adopted by chains in the early stages of adsorption, in fact, differ from those assumed at $t^* \gg 1$, and the energy landscape of interfacial chains is often bimodal also after prolonged annealing.[44] If the macromolecular architecture permits crystallization, annealing above T_g provides sufficient mobility to start crystallization. Chains far from the interfaces can form ordered structures via an outset entropic loss required for the formation of stems, which then migrate toward the crystal growth front. On the contrary, interfacial chains start to reduce their free energy via adsorption. Larger adsorption degrees, that is, larger enthalpy gain per surface unit, however, yield to an increase in the barrier to overcome before accessing the nearest available state of reduced free energy; the system gets thus trapped in a metastable noncrystalline state with an extremely long lifetime. Consequently, chains in the Guiselin brushes are expected to have tremendously low growth rates, corresponding to the lack of crystallization within reasonable time scales, in line with our experimental observation. These observations are valid in the case of capped films, a confinement geometry that is a reliable benchmark for nanocomposites,[45] where the only source for enhancement in segmental mobility is the excess in interfacial free volume, arising from packing frustration.[46−48]

In conclusion, we demonstrated that an analysis of the time dependence of the dielectric strength permits a quantitative analysis of the interplay between crystallization and irreversible chain adsorption in ultrathin polymer films. We verified that, in these systems, the slowing down in the crystallization kinetics

dx.doi.org/10.1021/mz300641x | ACS Macro Lett. 2013, 2, 168−172

cannot be rationalized by a mere reduction in segmental mobility (increase in T_g), but it is governed by the finite nuclei density. For samples thinner than twice the thickness of the layer irreversibly adsorbed onto the metallic surface, crystallization did not take place within the experimental time, that is, crystallization was severely inhibited or the growth rate dropped by more than 3 orders of magnitude for samples thinner than twice the thickness of the layer irreversibly adsorbed onto the metallic surface. We explain these findings considering that chain adsorption lowers the probability for the occurrence of the segment fluctuations required for the formation of crystalline structures.

■ ASSOCIATED CONTENT

Supporting Information

Supplementary experimental methods. Thickness dependence of the nucleation time, t_N, of the largest drop in dielectric strength G and of the cold crystallization temperature. This material is available free of charge via the Internet at http://pubs.acs.org.

■ AUTHOR INFORMATION

Corresponding Author

*E-mail: snapolit@ulb.ac.be.

Notes

The authors declare no competing financial interest.

■ ACKNOWLEDGMENTS

B.V. and M.W. acknowledge financial support from the Research Council of the KU Leuven, Project No. OT/11/065, and financial support from FWO (Fonds Wetenschappelijk Onderzoeks−Vlaanderen), Project G.0642.08. The authors acknowledge Gabin Gbabode for performing the XRD measurements. S.N. acknowledges Günter Reiter, Wenbing Hu, and Kari Dalnoki-Veress for fruitful discussions.

■ REFERENCES

(1) Grigoriadis, C.; Duran, H.; Steinhart, M.; Kappl, M.; Butt, H. J.; Floudas, G. *ACS Nano* **2011**, *5*, 9208.
(2) Liu, Y. X.; Chen, E. Q. *Coord. Chem. Rev.* **2010**, *254*, 1011.
(3) Asada, M.; Jiang, N.; Sendogdular, L.; Gin, P.; Wang, Y.; Endoh, M. K.; Koga, T.; Fukuto, M.; Schultz, D.; Lee, M.; Li, X.; Wang, J.; Kikuchi, M.; Takahara, A. *Macromolecules* **2012**, *45*, 7098.
(4) Despotopoulou, M. M.; Miller, R. D.; Rabolt, J. F.; Frank, C. W. *J. Polym. Sci., Part B: Polym. Phys.* **1996**, *34*, 2335.
(5) Despotopoulou, M. M.; Frank, C. W.; Miller, R. D.; Rabolt, J. F. *Macromolecules* **1996**, *29*, 5797.
(6) Massa, M. V.; Dalnoki-Veress, K.; Forrest, J. A. *Eur. Phys. J. E* **2003**, *11*, 191.
(7) Capitan, M. J.; Rueda, D. R.; Ezquerra, T. A. *Macromolecules* **2004**, *37*, 5653.
(8) Frank, C. W.; Rao, V.; Despotopoulou, M. M.; Pease, R. F. W.; Hinsberg, W. D.; Miller, R. D.; Rabolt, J. F. *Science* **1996**, *273*, 912.
(9) Paeng, K.; Swallen, S. F.; Ediger, M. D. *J. Am. Chem. Soc.* **2011**, *133*, 8444.
(10) Alvarez, C.; Sics, I.; Nogales, A.; Denchev, Z.; Funari, S. S.; Ezquerra, T. A. *Polymer* **2004**, *45*, 3953.
(11) Fukao, K.; Miyamoto, M. *Phys. Rev. Lett.* **1997**, *79*, 4613.
(12) Napolitano, S.; Prevosto, D.; Lucchesi, M.; Pingue, P.; D'Acunto, M.; Rolla, P. *Langmuir* **2007**, *23*, 2103.
(13) Flores, A.; Ania, F.; Arribas, C.; Ochoa, A.; Scholtyssek, S.; Balta-Calleja, F. J.; Baer, E. *Polymer* **2012**, *53*, 3986.
(14) Jukes, P. C.; Das, A.; Durell, M.; Trolley, D.; Higgins, A. M.; Geoghegan, M.; Macdonald, J. E.; Jones, R. A. L.; Brown, S.; Thompson, P. *Macromolecules* **2005**, *38*, 2315.
(15) Bertoldo, M.; Labardi, M.; Rotella, C.; Capaccioli, S. *Polymer* **2010**, *51*, 3660.
(16) Napolitano, S.; Wübbenhorst, M. *J. Phys. Chem. B* **2007**, *111*, 5775.
(17) Napolitano, S.; Wübbenhorst, M. *J. Non-Cryst. Solids* **2007**, *353*, 4357.
(18) Napolitano, S.; Wübbenhorst, M. *Macromolecules* **2006**, *39*, 5967.
(19) Rotella, C.; Napolitano, S.; Vandendriessche, S.; Valev, V. K.; Verbiest, T.; Larkowska, M.; Kucharski, S.; Wübbenhorst, M. *Langmuir* **2011**, *27*, 13533.
(20) Napolitano, S.; Wübbenhorst, M. *Nat. Commun.* **2011**, *2*, 260.
(21) Yin, H.; Napolitano, S.; Schoenhals, A. *Macromolecules* **2012**, *45*, 1652.
(22) Rotella, C.; Wübbenhorst, M.; Napolitano, S. *Soft Matter* **2011**, *7*, 5260.
(23) Rotella, C.; Napolitano, S.; De Cremer, L.; Koeckelberghs, G.; Wübbenhorst, M. *Macromolecules* **2010**, *43*, 8686.
(24) Reiter, G.; Sommer, J. U. *Phys. Rev. Lett.* **1998**, *80*, 3771.
(25) Massa, M. V.; L., C. J.; Dalnoki-Veress, K. *Phys. Rev. Lett.* **2006**, *97*, 247802.
(26) Massa, M. V.; Dalnoki-Veress, K. *Phys. Rev. Lett.* **2004**, 92.
(27) Schultz, J. M. *Macromolecules* **1996**, *29*, 3022.
(28) Napolitano, S.; Wübbenhorst, M. *J. Phys.: Condens. Matter* **2007**, *19*, 205121.
(29) Wang, Y.; Rafailovich, M.; Sokolov, J.; Gersappe, D.; Araki, T.; Zou, Y.; Kilcoyne, A. D. L.; Ade, H.; Marom, G.; Lustiger, A. *Phys. Rev. Lett.* **2006**, *96*, 083904.
(30) Palys, L. H.; Phillips, P. J. *J. Polym. Sci., Part B: Polym. Phys.* **1980**, *18*, 829.
(31) Frank, B.; Gast, A. P.; Russell, T. P.; Brown, H. R.; Hawker, C. *Macromolecules* **1996**, *29*, 6531.
(32) Einstein, A. *Investigation of the Theory of Browinan Motion*; Dover: New York, 1956.
(33) Ren, Y. J.; Huang, Z.; Hu, W. B. *J. Macromol. Sci., Part B: Phys.* **2012**, *51*, 2341.
(34) Ren, Y. J.; Gao, H. H.; Hu, W. B. *J. Macromol. Sci., Part B: Phys.* **2012**, *51*, 1548.
(35) Flores, A.; Balta-Calleja, F. J.; Di Marco, G.; Sturniolo, S.; Pieruccini, M. *Polymer* **2011**, *52*, 3155.
(36) Koga, T.; Jiang, N.; Gin, P.; Endoh, M. K.; Narayanan, S.; Lurio, L. B.; Sinha, S. K. *Phys. Rev. Lett.* **2011**, *107*, 225901.
(37) Harton, S. E.; Kumar, S. K.; Yang, H. C.; Koga, T.; Hicks, K.; Lee, E.; Mijovic, J.; Liu, M.; Vallery, R. S.; Gidley, D. W. *Macromolecules* **2010**, *43*, 3415.
(38) Guiselin, O. *Europhys. Lett.* **1991**, *17*, 225.
(39) Ligoure, C.; Leibler, L. *J. Phys.* **1990**, *51*, 1313.
(40) Zajac, R.; Chakrabarti, A. *Phys. Rev. E* **1995**, *52*, 6536.
(41) Strobl, G. *The Physics of Polymers*, 3rd ed.; Springer: Heidelberg, 2007.
(42) Larini, L.; Leporini, D. *J. Chem. Phys.* **2005**, *123*, 144907.
(43) Granick, S. *Eur. Phys. J. E* **2002**, *9*, 421.
(44) Schneider, H. M.; Frantz, P.; Granick, S. *Langmuir* **1996**, *12*, 994.
(45) Rittigstein, P.; Priestley, R. D.; Broadbelt, L. J.; Torkelson, J. M. *Nat. Mater.* **2007**, *6*, 278.
(46) Napolitano, S.; Pilleri, A.; Rolla, P.; Wübbenhorst, M. *ACS Nano* **2010**, *4*, 841.
(47) Napolitano, S.; Rotella, C.; Wübbenhorst, M. *ACS Macro Lett.* **2012**, *1*, 1189.
(48) Boucher, V. M.; Cangialosi, D.; Yin, H. J.; Schonhals, A.; Alegria, A.; Colmenero, J. *Soft Matter* **2012**, *8*, 5119.